HHS Public Access

Author manuscript

Neuroradiology. Author manuscript; available in PMC 2021 July 18.

Published in final edited form as:

Neuroradiology. 2021 June ; 63(6): 913–924. doi:10.1007/s00234-020-02614-6.

Changes in brain functional connectivity and cognition related to white matter lesion burden in hypertensive patients from SPRINT

Chintan Shah[1,3], **Dhivya Srinivasan**[1,2], **Guray Erus**[1,2], **James E. Schmitt**[1], **Adhish Agarwal**[4], **Monique E. Cho**[4], **Alan J. Lerner**[5], **William E. Haley**[6], **Manjula Kurella Tamura**[7,8], **Christos Davatzikos**[1,2], **Robert N. Bryan**[9], **Yong Fan**[1,2], **Ilya M. Nasrallah**[1,2]

[1]Department of Radiology, University of Pennsylvania, Philadelphia, PA, USA

[2]Center for Biomedical Image Computing and Analytics, University of Pennsylvania, PA Philadelphia, USA

[3]Department of Radiology, Imaging Institute, Cleveland Clinic, 9500 Euclid Ave, Mail code L10-428, Cleveland, OH 44195, USA

[4]Division of Nephrology and Hypertension, University of Utah, Salt Lake City, UT, USA

[5]University Hospitals Cleveland Medical Center, Department of Neurology, Case Western Reserve University, Cleveland, OH, USA

[6]Department of Nephrology and Hypertension, Mayo Clinic, Jacksonville, FL, USA

[7]Division of Nephrology, Stanford University, Palo Alto, CA, USA

[8]VA Palo Alto Geriatric Research and Education Clinical Center, Palo Alto, CA, USA

[9]Dell Medical School, Department of Diagnostic Medicine, University of Texas at Austin, Austin, TX, USA

Abstract

Chintan Shah shahc2@ccf.org.

Supplementary Information The online version contains supplementary material available at https://doi.org/10.1007/s00234-020-02614-6.

Data availability Clinical, demographic, and cognitive data, as well as structural MRI and fMRI metrics are maintained by the SPRINT coordinating center (www.sprinttrial.org). Data were processed using FSL (FMRIB Software Library, FMRIB, Oxford, UK), and MATLAB (MathWorks, Natick, MA). Anonymized data used in this manuscript will be shared by reasonable request from any qualified investigator for 5 years after the date of publication, with relevant associated code, once data is cleared for release by the trial coordinating center (date to be determined).

Compliance with ethical standards

Competing interests The authors declare no relevant financial or other conflicting interests. RN Bryan declares equity in Galileo CDS, Inc. (Founder and Chairman).

Ethics approval All procedures performed in studies involving human participants were in accordance with the ethical standards of the institutional and/or national research committee and with the 1964 Helsinki declaration and its later amendments or comparable ethical standards.

Consent to participate Informed consent was obtained from all individual participants included in the study.

Purpose—Hypertension is a risk factor for cognitive impairment; however, the mechanisms leading to cognitive changes remain unclear. In this cross-sectional study, we evaluate the impact of white matter lesion (WML) burden on brain functional connectivity (FC) and cognition in a large cohort of hypertensive patients from the Systolic Blood Pressure Intervention Trial (SPRINT) at baseline.

Methods—Functional networks were identified from baseline resting state functional MRI scans of 660 SPRINT participants using independent component analysis. WML volumes were calculated from structural MRI. Correlation analyses were carried out between mean FC of each functional network and global WML as well as WML within atlas-defined white matter regions. For networks of interest, voxel-wise-adjusted correlation analyses between FC and regional WML volume were performed. Multiple variable linear regression models were built for cognitive test performance as a function of network FC, followed by mediation analysis.

Results—Mean FC of the default mode network (DMN) was negatively correlated with global WML volume, and regional WML volume within the precuneus. Voxel-wise correlation analyses revealed that regional WML was negatively correlated with FC of the DMN's left lateral temporal region. FC in this region of the DMN was positively correlated to performance on the Montreal Cognitive Assessment and demonstrated significant mediation effects. Additional networks also demonstrated global and regional WML correlations; however, they did not demonstrate an association with cognition.

Conclusion—In hypertensive patients, greater WML volume is associated with lower FC of the DMN, which in turn is related to poorer cognitive test performance.

Trial registration—NCT01206062

Keywords

Hypertension; Functional connectivity; White matter lesions; Cognitive impairment

Introduction

Hypertension is well-known to be one of the most important risk factors for stroke [1, 2], as well as an independent risk factor for cognitive impairment [3] and Alzheimer's disease (AD) [4]. Aside from strokes, the most established imaging biomarkers of hypertension in the brain are volume of white matter lesions (WMLs) and brain atrophy [4, 5]. WMLs are foci of high signal intensity on T2-weighted images. Pathological correlation studies have demonstrated that WMLs are associated with chronic hypoperfusion and small vessel ischemic disease [6, 7]. WMLs are associated with several cerebrovascular risk factors but most strongly to hypertension, with studies suggesting decreased progression with hypertension treatment [5, 8, 9]. However, it remains unclear how WMLs affect functional brain networks and impact cognitive function in the setting of hypertension. The 2016 AHA statement on the impact of hypertension on cognitive function [4] concluded that the mechanism of how hypertensive changes lead to cognitive impairment is a key question for further study.

Resting state functional MRI (rs-fMRI) is a noninvasive tool to measure blood oxygenation level-dependent (BOLD) signals that can be used to investigate changes in brain functional connectivity (FC). Temporally correlated regions of low-frequency signal fluctuations in the resting brain on BOLD fMRI have shown reproducible, robust patterns that define intrinsic resting state functional networks [10]. Although the specific anatomic pathways within functional networks are not fully known, portions of these networks are linked in part via specific WM structural pathways [11] and FC may be disrupted by damage to these pathways [12]. Several resting state functional networks have been linked to cognitive function, most prominently the default mode network (DMN), which is disrupted in patients with AD [13]. However, only a few small studies have directly assessed FC in hypertensive patients. These studies found decreased FC within the DMN and frontoparietal networks in hypertensive patients [14, 15].

A subset of participants from the recently completed Systolic Blood Pressure Intervention Trial (SPRINT) [16] underwent multimodal brain MRI at baseline. The SPRINT showed that participants in the intensive blood pressure treatment group had a smaller increase in WML volume at follow-up [9] and a lower risk of mild cognitive impairment [17] compared to the standard treatment. Together, these findings suggest that increases in WML in hypertensive patients may be related to cognitive dysfunction. However, the mechanisms underlying translation of small vessel ischemic disease to neural impairment remain unclear. In the current study, we utilize the baseline functional neuroimaging data from the SPRINT to investigate the relationship between WML burden and functional brain networks in the setting of hypertension. We hypothesized that participants with greater WML volume would demonstrate decreased FC within intrinsic resting state functional networks, and that this would be related to poorer cognitive test performance.

Methods

Standard protocol approvals and patient consents

Institutional review boards at all clinical sites participating in the SPRINT approved the trial protocol for enrollment and data acquisition, and all participants signed written informed consent. SPRINT was sponsored by the National Institutes of Health.

Study sample

SPRINT is a large multi-center, randomized, controlled, open-label trial which randomized patients to intensive systolic blood pressure (SBP) target (< 120 mmHg) or standard SBP target (< 140 mmHg) blood pressure management [16]. The current cross-sectional study utilizes imaging, clinical, and cognitive data from a subset of the SPRINT cohort at baseline. SPRINT enrolled 9361 nondiabetic adults over age 50 with SBP > 130 and an elevated cardiovascular risk profile. Prior stroke, diabetes mellitus, and recent cardiovascular event within 3 months were among the study exclusion criteria. The full inclusion and exclusion criteria have been previously published [16]. The SPRINT MRI substudy included participants from the larger study who were within 1.5-h driving distance of one of seven MRI centers in the USA and who did not have MRI-related exclusion factors, such as a non-MRI compatible device or foreign object or claustrophobia. Additional participants were

also recruited from the SPRINT ancillary study MIND the Kidneys, which was designed to augment the MRI group with participants with chronic kidney disease [18].

A total of 786 participants underwent MRI at baseline, of which 18 did not have rs-fMRI acquired due to technical or patient-related factors. Of the 768 participants with rs-fMRI, 14 were excluded due to the presence of structural lesions, such as large infarcts or tumors that could directly affect brain networks, 9 did not have available or intact demographic or cognitive data, 4 did not pass structural imaging quality control (1 missing image data, 1 poor-quality raw images, 2 failed processing), and 81 did not pass functional imaging quality control (75 excessive motion, 4 poor-quality raw images, 2 failed registration to structural images). The final cohort for this study included 660 participants.

MRI data acquisition

MRI scans were performed across eleven centers utilizing 3-T scanners from three different vendors (Siemens, Munich, Germany; Philips, Best, the Netherlands; GE Healthcare, Cleveland, OH) using 12-channel receive head coils. The MRI scanning protocol included the following sagittal 1-mm isotropic structural sequences: T1-weighted MPRAGE, T2-weighted FLAIR, T2-weighted fast spin echo, previously described [9]. An rs-fMRI scan was acquired using an axial BOLD echo planar imaging sequence, with TR/TE 2000/25 ms, isotropic 3.5-mm voxels, and 120 volumes.

Cognitive assessment

All participants underwent the Montreal Cognitive assessment (MoCA), the Digit Symbol Coding (DSC) test, and the Logical Memory (LM) test. Full details on the cognitive assessment protocol are available at the trial website (http://www.sprinttrial.org).

Structural image processing

Structural imaging results for SPRINT were previously reported [9]. Briefly, intracranial tissues were extracted using multi-atlas skull stripping [19] and segmented using a multi-atlas label fusion method [20]. WML were identified using a deep learning–based classification model, built on the UNet architecture with the internal convolutional network layers replaced with an Inception ResNet architecture, as described previously [9]. The model was trained on a separate set of cases with expert-delineated WML. Quality inspection of WML classification was performed by a neuroradiologist at the MRI reading center. WM regions of interest (ROIs) were identified based on registration to the Johns Hopkins University “Eve” atlas [21]. All supratentorial non-cortical ROIs from this atlas were included, for a total of 49 paired (bilateral) regions. WML volume was calculated within each region, and global WML burden was calculated as total volume of WML within 49 bilateral supratentorial ROIs.

Functional image processing

Resting state fMRI data was pre-processed in standard fashion, including removal of first 6 volumes for signal equilibration, slice time correction, and motion correction. Motion correction was applied utilizing the FMRIB Software Library (FSL) application MCFLIRT, which provides an output metric of the relative displacement between time frames [22].

Scans with gross motion were initially excluded if any motion exceeded 3.5 mm. Participants were then excluded from analysis if the mean relative displacement was greater than 0.3 mm [23, 24]. Global mean signal was regressed out as a well-known surrogate for motion and physiologic noise, as were additional nuisance variables including 6 motion parameters and white matter and cerebrospinal fluid signal from tissue segmentations. This was followed by spatial smoothing (6 mm full width half maximum), temporal bandpass filtering (0.01–0.1 Hz), and registration into Montreal Neurological Institute template space at 4-mm isotropic resolution. Functional brain networks were identified and extracted using an independent component analysis (ICA) approach [25]. Group-level ICA was performed using Melodic [26], with a standard low-order dimensionality of 20 components [27]. Subject-level-independent components were then calculated using group information-guided ICA (GIGICA) [28], which outputs a spatial map and time course for each component. Subject-specific networks derived using this method have been shown to have better independence and higher spatial and temporal accuracy [28], and the GIGICA has been shown to have greater performance for artifact removal [29] and individual subject classification [30–32]. Subject-level within-network FC *z*-score maps were calculated for each network via temporal correlation with the extracted time course for each component from the GIGICA, and subsequently applying Fisher's R to Z transform. Mean connectivity score (MCS) was calculated for each network in each participant as the participant's average within-network FC within a 3D mask of the group network, as described in other studies [33]. The network masks were created by thresholding the group ICA spatial maps, where the threshold = 0.3× maximum intensity (maximum value of the robust range, 2nd to 98th percentile) for each component [33].

To assess the integrity of neurovascular coupling, the resting state fluctuation of amplitude (RSFA) was calculated as the temporal standard deviation of the resting state BOLD signal [34], which has been reported to be a more reliable measure than breath-hold-based cerebrovascular reactivity for studies in which there is a large age range [34].

Group-level statistical analyses

We hypothesized that greater WML burden would be related to disruptions in brain functional networks, and that these disruptions would be associated with cognitive changes. As an initial quality control step, the correlation between RSFA and WML volume was assessed to ensure that any relationship between WML and FC was not being spuriously driven by systematic alterations in neurovascular coupling. Correlations were then performed between total supratentorial WML burden and overall within-network connectivity for each network, to identify networks of interest. This was followed by the identification of (1) specific WM regions in the brain which WML load was related to the overall connectivity for each network, and (2) regions of each network where within-network connectivity was related to WML within these WM regions. Cognitive test performance was then modeled including overall network FC, and FC within these WML-related regions of the network as a predictor, followed by mediation analysis. Given the right-skewed nature of the WML distribution, a cube root transformation as first applied to the WML values prior to any statistical analysis, which is similar to a log transformation but can accommodate values of zero. Statistical analyses were performed using MATLAB

(MathWorks, Natick, MA), and mediation analysis was performed in R (R Project for Statistical Computing [http://www.r-project.org]).

Correlation between mean overall network FC and total WML

As an initial screening step to identify networks of interest, mean connectivity score for each network was calculated and correlated to total supratentorial WML volume. Networks in which there was a significant correlation ($p < 0.05$, uncorrected) were identified as networks of interest. Multiple comparison correction was applied in the following more rigorous correlation step.

Correlation between mean overall network FC and regional WML

To determine WM regions of the brain where WML volume was related to average within-network FC, correlation was performed between WML volume within 49 supratentorial ROIs and MCS of resting state networks. Bilateral ROI WML volume was used for all networks aside from lateralized networks, in which ipsilateral ROI WML volume was used. False discovery rate (FDR) correction for multiple comparisons was performed.

For each network of interest that demonstrated significant correlation between MCS and WML within specific WM ROIs, the total WML volume within these significant ROIs was calculated as the regional WML (rWML) volume for this network. To ensure the relationship held after accounting for potential confounders, multiple variable linear regression was then performed for network MCS with rWML as the primary predictor, and adjusters including gray matter ratio (total gray matter volume normalized to intracranial volume), age, gender, and race. Gray matter ratio (GMR) was included as an adjuster to account for alterations in FC related to gray matter volume. To assess for site- or scanner-related variations in imaging results, the full model also adjusted for site as a binarized set of 9 variables, one for each site with greater than 3 participants. Two additional sites had 3 participants each, and variables were not included for these sites as the low number of participants precluded an accurate statistical estimate of their contribution to the shared variance. The site variables were removed from the final model if not found to be significant adjusters, and networks in which site was a significant predictor of MCS were excluded from subsequent analysis. Scatter plots were created for MCS as a function of rWML.

Correlation between regional network FC and WML

For each remaining resting state network of interest that demonstrated correlations to regional WML, to determine the brain regions within the network where FC was related to rWML, voxel-wise correlation was performed between participant-level FC maps and their corresponding rWML, adjusted for gray matter ratio, age, gender, and race. This produced a t score spatial map of correlation between local within-network FC and rWML burden. Correlation t score maps were thresholded at $t = 2.58$ ($p < 0.01$, uncorrected). Monte Carlo simulation was then performed to determine the cluster size representative of a threshold of $p < 0.0001$, family wise error (FWE)-corrected. Significant clusters represent the regions within a network where FC is correlated to rWML.

Subsequently, for each network of interest, the average FC was calculated for each participant within significant clusters, including those clusters in which the direction of correlation matched that of the overall network MCS-rWML correlation. This is referred to herein as the WML-related cluster connectivity (WCC) and represents the average within-network connectivity specifically in brain regions where the within-network FC is related to WML burden in the cohort.

Multiple variable linear regression was repeated as above, now with network WCC as the outcome, rWML as the primary predictor, and adjustment for gray matter ratio, age, gender, and race. Scatter plots were created for WCC as a function of rWML, for visualization purposes.

Neurocognitive significance of WML-related changes in FC

For networks of interest from the above analysis, further analysis was undertaken to determine the relationship of FC with cognitive function. First, multiple variable linear regression models were built for performance on the MoCA, LM (delayed recall), and DSC tests. Model predictors included mean connectivity score for the networks of interest, and demographic variables (age, gender, race). For cognitive tests where mean connectivity score of a network demonstrated a significant correlation ($p < 0.05$), regression models were created again in similar fashion, replacing mean connectivity scores with WCC of the significant network, to determine whether connectivity in these specific network regions are driving the relationship with cognitive test performance.

In order to further investigate the causal relationships between imaging and cognitive variables, the data were imported into R for mediation analysis [35–37]. Conditional process models were constructed that examined whether the rWML exerted its influences on cognitive performance via disruptions to functional connectivity. Specifically, two linear models were constructed, one that describes the conditional distribution of the mediator (WCC) given the independent variable (rWML), and the second is an outcome model describing the conditional distribution of cognitive performance given the influences of both WCC and rWML; these models were then examined simultaneously to quantify the mediation effect. Models were also adjusted for age, gender, race, and gray matter ratio. We estimated the average causal mediation effects (ACME), which is the indirect effect of rWML exerted through the WCC. An estimate of the average direct effect (ADE), as well as total effect, was also calculated. Parameters were estimated via bootstrap with 10,000 replications.

Results

Demographic and clinical data of the 660-participant cohort are presented in Table 1. The cohort was similar to the main SPRINT [16] in terms of age and gender makeup, with slightly smaller proportion of Hispanic participants and greater proportion of White participants. There was a greater proportion of subjects with chronic kidney disease in this cohort relative to SPRINT (36% vs. 28%); however, there is no apparently clinically important difference in overall estimated glomerular filtration rate (69 vs. 72 ml/min/1.72 m^2). Twenty independent components were identified using group ICA. Five of these

components were deemed to represent artifact or noise related to vasculature, motion, or CSF by visual inspection, with the remaining 15 representing intrinsic resting state brain networks. These are displayed in Figure S1. Some canonical networks were identified across multiple components such as the sensorimotor network and the DMN. Others were combined, for example, a component including brain regions in the temporal lobes, insula, and cingulate cortex, likely reflected a conglomerate component encompassing auditory, salience, and language networks (ASLN). RSFA did not demonstrate a correlation with WML for any network of interest ($p > 0.05$).

Correlation between mean overall network FC and total WML

Global WML volume demonstrated a significant correlation with the mean connectivity score of six of the 15 networks (Table S1). These represented the DMN ($R = -0.076$; $p = 0.0431$), ASLN ($R = -0.1279$; $p = 0.0006$), left frontoparietal network (LFPN; $R = 0.0745$; $p = 0.0474$), posterior DMN (pDMN; $R = -0.0901$; $p = 0.0165$), dorsal frontal network (DFN; $R = 0.0773$; $p = 0.0472$), and basal ganglia network (BGN; $R = -0.0841$; $p = 0.0307$).

Correlation between mean overall network FC and regional WML

Significant correlations between network MCS and regional WML are demonstrated in Table 2 for networks of interest. MCS of the ASLN was significantly negatively correlated to WML volume within the posterior thalamic radiations and thalamus, and corpus callosum (including genu, body, splenium, and tapetum). Overall, DMN connectivity was related negatively to WML within the precuneus. LFPN connectivity demonstrated a positive correlation with WML within the cingulum. Connectivity of the pDMN demonstrated a negative relationship with WML in the posterior corona radiata. WML within the fornix was negatively related to FC in the DFN and BGN.

The total WML within above noted ROIs was calculated for each subject as the rWML for that network. Multiple variable linear regression models with adjusters demonstrated that site variables were significant covariates for the model of BG MCS, but not for other networks. BGN was removed from subsequent analysis. For the other networks, models were recalculated without site variables to avoid reducing statistical power. After adjustment, rWML was a significant predictor of MCS for ASLN, DMN, LFPN, and DFN ($p < 0.05$), but not for pDMN. Full regression model statistics are available in Table S2. Gray matter ratio was a significant adjuster for the DMN, and Black and Hispanic races were significant adjusters for the DFN. Otherwise, no adjusters were significant.

Correlation between regional network FC and WML

In the DMN (Fig. 1a), clusters of significant correlation are seen (Fig. 1b), the largest of which is a negative correlation in the left lateral temporal cortex region of the DMN. A small cluster of positive correlation is also seen in the left superior temporal lobe. Displayed regions (clusters) represent regions of the respective networks where within-network FC is related to rWML. Correlation maps for remaining networks are displayed in Figure S2. In the ASLN, significant negative correlations are seen in the cingulate cortex and the bilateral insular region, as well as the right parietal lobe. The LFPN demonstrates positive regions of

correlation within the left frontal and parietal cortex, as well as a smaller region in the contralateral frontal lobe. The pDMN shows negative clusters of correlation in the left parietal and dorsal prefrontal cortex. The DFN shows a large cluster of negative correlation involving the dorsal frontal lobes and smaller clusters in the bilateral striatum, as well as a curvilinear area of positive correlation along the anterior margin of the frontal lobes which may reflect artifact.

Masks of these clusters for each network of interest were created and used to calculate the WCC for each participant. Multiple variable linear regression showed that rWML was a significant predictor of WCC for all networks (Table S3). Age was a significant adjuster for ASLN WCC, and age and Black race were significant adjusters for the DFN.

Neurocognitive significance of WML-related changes in FC

Multiple variable regression models of performance on the MoCA, LM, and DSC tests, including MCS for all networks of interest as predictors, are shown in Table 3. DMN mean connectivity was significantly correlated with MoCA performance ($p = 0.0025$) after adjusting for GMR, age, gender, and race, but MCS of the other networks of interest were not significant predictors of MoCA performance. A second regression model was built for MoCA performance substituting all mean connectivity metrics with DMN WCC only (Table 4), which also demonstrated a significant correlation ($p = 0.0040$).

DSC test performance was not significantly related to mean connectivity in any network of interest, although there was a negative trend for the ASLN ($p = 0.0624$). Delayed recall on the LM test did not demonstrate significant correlations with the connectivity of any networks of interest.

Full model statistics are available in Table S4. For all three cognitive tests, age was a significant negative adjuster, and white race was a significant positive adjuster. GMR was a significant positive adjuster for the DSC and LM tests, as was female gender was for the LM test.

Conditional process modeling results are summarized in Fig. 2. The relationships between default mode network rWML and MoCA were significantly mediated via the WCC (bootstrap p value 0.0056). Increasing rWML negatively influenced regional FC in the DMN, which in turn disrupted the positive influence of higher FC on cognition. Similar but less pronounced findings were observed for DMN MCS (bootstrap p value 0.0250).

Discussion

Our results indicate that higher WML burden in hypertensive patients is associated with weakened overall connectivity of several cortical networks, including the DMN and ASLN, and increased connectivity in others, such as the LFPN. However, only the FC disruptions in the DMN were found to be related to cognitive function via multiple variable regression and mediation analysis.

The DMN is a collection of brain regions which demonstrate coordinated activity at rest, but are also modulated during a variety of cognitive tasks, especially those involving self-

generated thought [13, 38]. FC of the DMN has been shown to be disrupted in several disease states including AD [13] and schizophrenia [39]. In this study, negative correlations with WML volume were seen in specific regions of the DMN, the largest cluster being in the lateral temporal lobe, a region of the DMN that is involved in semantic processing and memory retrieval [38]. FCs in these regions, as well as overall DMN connectivity, were found to mediate the relationship between WML and MoCA performance. Thus, in hypertensive patients, greater WML burden is associated with lower overall and regional DMN connectivity, which in turn is associated with worse MoCA performance.

ICA separates networks to varying degrees depending on the underlying population, analysis methodology, and dimensionality chosen [27]. The ASLN identified by ICA in our cohort includes brain regions in the temporal lobes, insula, and cingulate cortex, and likely reflects a conglomerate component encompassing auditory, language, and salience networks. The network regions that demonstrated negative correlations with WML include the bilateral insula and cingulate gyrus, regions most typically associated with the salience network. Connectivity within these regions of the ASLN demonstrated a nonsignificant trend towards correlation with performance on the DSC test, which is a measure of processing speed and working memory [40]. The mean connectivity of the ASLN was also significantly related to lesion burden in large WM tracts such as the corpus callosum.

The LFPN and its contralateral paired network are sometimes referred to as the executive control networks. The DMN, executive control networks, and salience network have been proposed to function together to modulate internal cognitive processes, externally directed attentional processes, and switching between them, respectively [41]. FC in the LFPN demonstrated significantly positive correlation with total WML; however, it was not related to performance on these cognitive tests. This may reflect a compensatory mechanism of increased within-network connectivity in the LFPN in response to the deficits in the DMN and ASLN, greater resilience of this network to injury via WML, and/or decreased sensitivity of the available cognitive assessments to changes of this network.

The DFN demonstrated an overall positive relationship with total WML; however, lesion load in the only significant white matter region demonstrated a negative correlation. This underscores that the effects of WML vary by location, and can result in differing effects at the local or global network level. These differing effects likely obscure any overall relationship with clinically measurable cognitive changes.

Our models for performance on the MoCA, DSC, and LM cognitive tests also found that white race was a significantly positive adjuster for performance on all three tests. This is concordant with prior studies suggesting that race and ethnicity are important factors that influence appropriate cutoffs on cognitive tests [42–44].

Only a few studies have directly assessed alterations in FC in hypertensive patients [14, 15]. Son et al. [14] evaluated 37 patients with AD with and without hypertension, and found that DMN connectivity was disrupted in the hypertensive group; however, the presence of AD in the underlying cohort produces difficulty in extrapolating these results to hypertensive patients without AD. Li et al. [15] found that FC of the left frontoparietal network was

disrupted in 44 hypertensive patients relative to 40 normal controls, but did not find significant group differences in the DMN. Furthermore, left inferior parietal lobe FC was a mediating pathway between disrupted WM integrity and performance on the trail making test. Some differences between our results and this study are likely because of differing designs—we did not compare FC in hypertensive patients to normal controls but rather assessed FC alterations in relation to global and regional WML volume within a group of hypertensive patients. In a smaller study comparing 15 patients with WML to 15 healthy controls, Ding et al. [45] found disrupted connectivity within the auditory and visual network in patients with ischemic WML, as well as multiple alterations in between-network connectivity, which was not directly assessed in our study. Our results support and further these conclusions, demonstrating in a much larger hypertensive cohort that overall WML burden is related to network-level disruption and related cognitive dysfunction.

While this study may have benefitted from the inclusion of a control group of normotensive patients, such a group was not included in the design of SPRINT. However, the definition of normotension is debated, and SPRINT itself provided evidence for redefining hypertension thresholds in the 2017 ACC/AHA Hypertension Guidelines [46]. We did not adjust for the long-term severity of hypertension; however, estimating such a metric is difficult; measures such as current blood pressure, duration of hypertension, and number of antihypertensive medications may not provide a full picture of a patient's cumulative exposure to hypertension. In this study, we considered WML our primary exposure, utilizing it as a surrogate for how severely the patient's brain had been affected by hypertension. This approach allowed us to capture effects across the full spectrum of hypertension severity rather than using an arbitrary cutoff to dichotomize participants into groups. However, our findings are thus limited to those effects related to WM damage in the setting of hypertension and not other potential mechanisms such as direct neuronal loss or atrophy, and it is also uncertain if the results could be extrapolated to conditions where other pathologies contribute to development of WML. We found that several demographic variables influenced cognitive test performance and adjusted for these; however, it remains possible that additional unmeasured confounders exist that could influence both WML and cognition.

Technical limitations include the use of rs-fMRI to measure FC, as the BOLD response may be altered in hypertension. To address this issue, we calculated the RSFA as an indirect measure of neurovascular coupling and demonstrated that it was not related to WML in any network of interest. Thus, although this remains an important consideration with potential to reduce study power, it is unlikely to be systematically biasing our results. The acquisition of rs-fMRI data across multiple sites with several different scanner models likely reduced study power. Finally, the cross-sectional design of this study allowed us to characterize the relationship between greater WML burden and brain network function, but not how longitudinal changes in WML over time may affect brain networks, which will be the focus of future studies.

Conclusions

In this cross-sectional study of the SPRINT cohort at baseline, we have found that greater WML volume is related to lower FC of the DMN. Furthermore, WML-related disruptions in

this network were found to mediate poorer cognition as measured by the MoCA. These findings, in combination with prior SPRINT studies, suggest that preventing progression of WML may slow cognitive decline in hypertensive patients without cognitive impairment. Future work evaluating how these measures of network FC are altered longitudinally in hypertension will help understand the progression of hypertension-related brain disease and the impact of hypertension treatment.

Supplementary Material

Refer to Web version on PubMed Central for supplementary material.

Acknowledgments

Funding The Systolic Blood Pressure Intervention Trial is funded with Federal funds from the National Institutes of Health (NIH), including the National Heart, Lung, and Blood Institute (NHLBI); the National Institute of Diabetes and Digestive and Kidney Diseases (NIDDK); the National Institute on Aging (NIA); and the National Institute of Neurological Disorders and Stroke (NINDS), under Contract Numbers HHSN268200900040C, HHSN268200900046C, HHSN268200900047C, HHSN268200900048C, and HHSN268200900049C, and Inter-Agency Agreement Number A-HL-13-002-001. It was also supported in part with resources and use of facilities through the Department of Veterans Affairs. The SPRINT investigators acknowledge the contribution of study medications (azilsartan and azilsartan combined with chlorthalidone) from Takeda Pharmaceuticals International, Inc. All components of the SPRINT study protocol were designed and implemented by the investigators. The investigative team collected, analyzed, and interpreted the data. All aspects of manuscript writing and revision were carried out by the coauthors. The content is solely the responsibility of the authors and does not necessarily represent the official views of the NIH, the US Department of Veterans Affairs, or the United States Government. For a full list of contributors to SPRINT, please see the supplementary acknowledgement list: SPRINT Acknowledgment.

We also acknowledge the support from the following CTSAs funded by NCATS:

CWRU: UL1TR000439; OSU: UL1RR025755; U Penn: UL1RR024134 and UL1TR000003; Boston: UL1RR025771; Stanford: UL1TR000093; Tufts: UL1RR025752, UL1TR000073, and UL1TR001064; University of Illinois: UL1TR000050; University of Pittsburgh: UL1TR000005; UT Southwestern: 9U54TR000017-06; University of Utah: UL1TR000105-05; Vanderbilt University: UL1 TR000445; George Washington University: UL1TR000075; University of CA, Davis: UL1 TR000002; University of Florida: UL1 TR000064; University of Michigan: UL1TR000433; Tulane University: P30GM103337 COBRE Award NIGMS. CS partially supported by NIH T32 Training Grant EB004311 and Radiological Society of North America fellow research grant. MKT was supported by R01 DK092241.

Abbreviations

AD	Alzheimer’s disease
ASLN	Auditory, salience, and language network
BOLD	Blood oxygenation level-dependent
DMN	Default mode network
DSC	Digit Symbol Coding
FC	Functional connectivity
FDR	False discovery rate
FWE	Family wise error

GIGICA	Group information-guided independent component analysis
ICA	Independent component analysis
LFPN	Left frontoparietal network
LM	Logical Memory
MCS	Mean connectivity score
MoCA	Montreal Cognitive Assessment
pDMN	Posterior default mode network
ROI	Region of interest
RSFA	Resting state fluctuation of amplitude
rs-fMRI	Resting state functional magnetic resonance imaging
SBP	Systolic blood pressure
SPRINT	Systolic Blood Pressure Intervention Trial
WCC	White matter lesion-related cluster connectivity
WML	White matter lesion

References

1. Mozaffarian D, Benjamin EJ, Go AS, et al. (2016) Heart disease and stroke statistics-2016 update a report from the American Heart Association
2. Law MR, Morris JK, Wald NJ (2009) Use of blood pressure lowering drugs in the prevention of cardiovascular disease: meta-analysis of 147 randomised trials in the context of expectations from prospective epidemiological studies. BMJ 338:b1665
3. Reitz C, Tang MX, Manly J, Mayeux R, Luchsinger JA (2007) Hypertension and the risk of mild cognitive impairment. Arch Neurol 64:1734–1740 [PubMed: 18071036]
4. Iadecola C, Yaffe K, Biller J, Bratzke LC, Faraci FM, Gorelick PB, Gulati M, Kamel H, Knopman DS, Launer LJ, Saczynski JS, Seshadri S, Zeki al Hazzouri A, American Heart Association Council on Hypertension; Council on Clinical Cardiology; Council on Cardiovascular Disease in the Young; Council on Cardiovascular and Stroke Nursing; Council on Quality of Care and Outcomes Research; and Stroke Council (2016) Impact of hypertension on cognitive function: a scientific statement from the American Heart Association. Hypertension 68:e67–e94 [PubMed: 27977393]
5. Firbank MJ, Wiseman RM, Burton EJ, Saxby BK, O'Brien JT, Ford GA (2007) Brain atrophy and white matter hyperintensity change in older adults and relationship to blood pressure. Brain atrophy, WMH change and blood pressure. J Neurol 254:713–721 [PubMed: 17446997]
6. Fernando MS, Simpson JE, Matthews F, Brayne C, Lewis CE, Barber R, Kalaria RN, Forster G, Esteves F, Wharton SB, Shaw PJ, O'Brien JT, Ince PG (2006) White matter lesions in an unselected cohort of the elderly: molecular pathology suggests origin from chronic hypoperfusion injury. Stroke 37:1391–1398 [PubMed: 16627790]
7. Erten-Lyons D, Woltjer R, Kaye J, Mattek N, Dodge HH, Green S, Tran H, Howieson DB, Wild K, Silbert LC (2013) Neuropathologic basis of white matter hyperintensity accumulation with advanced age. Neurology 81:977–983 [PubMed: 23935177]
8. Dufouil C, Chalmers J, Coskun O, Besançon V, Bousser MG, Guillon P, MacMahon S, Mazoyer B, Neal B, Woodward M, Tzourio-Mazoyer N, Tzourio C, PROGRESS MRI Substudy Investigators

(2005) Effects of blood pressure lowering on cerebral white matter hyperintensities in patients with stroke: the PROGRESS (Perindopril Protection Against Recurrent Stroke Study) magnetic resonance imaging substudy. Circulation 112: 1644–1650 [PubMed: 16145004]

9. Nasrallah IM, Pajewski NM, Auchus AP et al. (2019) Association of intensive vs standard blood pressure control with cerebral white matter lesions. JAMA - J Am Med Assoc 322:524–534
10. Biswal B, Yetkin FZ, Haughton VM et al. (1995) Functional connectivity in the motor cortex of resting human brain using echoplanar MRI. Magn Reson Med 34:537–541 [PubMed: 8524021]
11. Van Den Heuvel MP, Mandl RCW, Kahn RS et al. (2009) Functionally linked resting-state networks reflect the underlying structural connectivity architecture of the human brain. Hum Brain Mapp 30:3127–3141 [PubMed: 19235882]
12. Lowe MJ, Beall EB, Sakaie KE, Koenig KA, Stone L, Marrie RA, Phillips MD (2008) Resting state sensorimotor functional connectivity in multiple sclerosis inversely correlates with transcallosal motor pathway transverse diffusivity. Hum Brain Mapp 29:818–827 [PubMed: 18438889]
13. Hafkemeijer A, van der Grond J, Rombouts SARB (1822) Imaging the default mode network in aging and dementia. Biochim Biophys Acta 2012:431–441
14. Son SJ, Kim J, Lee E, Park JY, Namkoong K, Hong CH, Ku J, Kim E, Oh BH (2015) Effect of hypertension on the resting-state functional connectivity in patients with Alzheimer's disease (AD). Arch Gerontol Geriatr 60:210–216 [PubMed: 25307953]
15. Li X, Liang Y, Chen Y, Zhang J, Wei D, Chen K, Shu N, Reiman EM, Zhang Z (2015) Disrupted frontoparietal network mediates white matter structure dysfunction associated with cognitive decline in hypertension patients. J Neurosci 35:10015–10024 [PubMed: 26157001]
16. SPRINT Research Group Wright JT, Williamson JD et al. (2015) A randomized trial of intensive versus standard blood-pressure control. N Engl J Med 373:2103–2116 [PubMed: 26551272]
17. Williamson JD, Pajewski NM, Auchus AP et al. (2019) Effect of intensive vs standard blood pressure control on probable dementia: a randomized clinical trial. JAMA - J Am Med Assoc 321:553–561
18. Tamura MK, Pajewski NM, Bryan RN et al. (2016) Chronic kidney disease, cerebral blood flow, and white matter volume in hypertensive adults. Neurology 86:1208–1216 [PubMed: 26920359]
19. Doshi J, Erus G, Ou Y, Gaonkar B, Davatzikos C (2013) Multiatlas skull-stripping. Acad Radiol 20:1566–1576 [PubMed: 24200484]
20. Doshi J, Erus G, Ou Y, Resnick SM, Gur RC, Gur RE, Satterthwaite TD, Furth S, Davatzikos C, Alzheimer's Neuroimaging Initiative (2016) MUSE: MUlti-atlas region segmentation utilizing ensembles of registration algorithms and parameters, and locally optimal atlas selection. Neuroimage 127: 186–195 [PubMed: 26679328]
21. Oishi K, Faria A, Jiang H, Li X, Akhter K, Zhang J, Hsu JT, Miller MI, van Zijl PCM, Albert M, Lyketsos CG, Woods R, Toga AW, Pike GB, Rosa-Neto P, Evans A, Mazziotta J, Mori S (2009) Atlas-based whole brain white matter analysis using large deformation diffeomorphic metric mapping: application to normal elderly and Alzheimer's disease participants. Neuroimage 46:486–499 [PubMed: 19385016]
22. Jenkinson M, Bannister P, Brady M, Smith S (2002) Improved optimization for the robust and accurate linear registration and motion correction of brain images. Neuroimage 17:825–841 [PubMed: 12377157]
23. Satterthwaite TD, Wolf DH, Loughead J, Ruparel K, Elliott MA, Hakonarson H, Gur RC, Gur RE (2012) Impact of in-scanner head motion on multiple measures of functional connectivity: relevance for studies of neurodevelopment in youth. Neuroimage 60:623–632 [PubMed: 22233733]
24. Power JD, Mitra A, Laumann TO et al. (2014) Methods to detect, characterize, and remove motion artifact in resting state fMRI. Neuroimage 84:320–341 [PubMed: 23994314]
25. Calhoun VD, Liu J, Adali T (2009) A review of group ICA for fMRI data and ICA for joint inference of imaging, genetic, and ERP data. Neuroimage 45:S163–S172 [PubMed: 19059344]
26. Beckmann CF, Smith SM (2004) Probabilistic independent component analysis for functional magnetic resonance imaging. IEEE Trans Med Imaging 23:137–152 [PubMed: 14964560]

27. Ray KL, McKay DR, Fox PM et al. (2013) ICA model order selection of task co-activation networks. Front Neurosci 7:237 [PubMed: 24339802]
28. Du Y, Fan Y (2013) Group information guided ICA for fMRI data analysis. Neuroimage 69:157–197 [PubMed: 23194820]
29. Du Y, Allen EA, He H et al. (2016) Artifact removal in the context of group ICA: a comparison of single-subject and group approaches. Hum Brain Mapp 37:1005–1025 [PubMed: 26859308]
30. Jing R, Li P, Ding Z, Lin X, Zhao R, Shi L, Yan H, Liao J, Zhuo C, Lu L, Fan Y (2019) Machine learning identifies unaffected first-degree relatives with functional network patterns and cognitive impairment similar to those of schizophrenia patients. Hum Brain Mapp 40:3930–3939 [PubMed: 31148311]
31. Jing R, Han Y, Cheng H, Han Y, Wang K, Weintraub D, Fan Y (2020) Altered large-scale functional brain networks in neurological Wilson's disease. Brain Imaging Behav 14:1445–1455 [PubMed: 31011947]
32. Wetherill RR, Rao H, Hager N, Wang J, Franklin TR, Fan Y (2019) Classifying and characterizing nicotine use disorder with high accuracy using machine learning and resting-state fMRI. Addict Biol 24:811–821 [PubMed: 29949234]
33. Wisner KM, Patzelt EH, Lim KO, MacDonald AW III (2013) An intrinsic connectivity network approach to insula-derived dysfunctions among cocaine users. Am J Drug Alcohol Abuse 39:403–413 [PubMed: 24200210]
34. Kannurpatti SS, Motes MA, Biswal BB, Rypma B (2014) Assessment of unconstrained cerebrovascular reactivity marker for large age-range FMRI studies. PLoS One 9:e88751
35. Development Core Team R (2020) R: A language and environment for statistical computing. R Foundation for Statistical Computing, Vienna
36. Imai K, Keele L, Yamamoto T Identification, inference and sensitivity analysis for causal mediation effects. 10.1214/10-STS321.
37. Hayes A. Introduction to mediation, moderation, and conditional process analysis. New York, NY Guilford 978–1-60918–230-4.
38. Andrews-Hanna JR, Smallwood J, Spreng RN (2014) The default network and self-generated thought: component processes, dynamic control, and clinical relevance. Ann N Y Acad Sci 1316:29–52 [PubMed: 24502540]
39. Calhoun VD, Maciejewski PK, Pearlson GD, Kiehl KA (2008) Temporal lobe and "default" hemodynamic brain modes discriminate between schizophrenia and bipolar disorder. Hum Brain Mapp 29:1265–1275 [PubMed: 17894392]
40. Jaeger J (2018) Digit symbol substitution test. J Clin Psychopharmacol 38:513–519 [PubMed: 30124583]
41. Menon V (2015) Salience network. In: Toga AW (ed) Brain Mapping: An Encyclopedic Reference, 2nd edn. Academic Press: Elsevier, pp 597–611
42. Sink KM, Craft S, Smith SC, Maldjian JA, Bowden DW, Xu J, Freedman BI, Divers J (2015) Montreal cognitive assessment and modified mini mental state examination in African Americans. J Aging Res 2015:1–6
43. Milani SA, Marsiske M, Cottler LB et al. (2018) Optimal cutoffs for the Montreal Cognitive Assessment vary by race and ethnicity. Alzheimer's Dement Diagnosis, Assess Dis Monit 10:773–781
44. Still CH, Pajewski NM, Chelune GJ, Rapp SR, Sink KM, Wadley VG, Williamson JD, Lerner AJ (2019) The association between the Montreal Cognitive Assessment and Functional Activity Questionnaire in the Systolic Blood Pressure Intervention Trial (SPRINT). Arch Clin Neuropsychol 34:814–824 [PubMed: 30517599]
45. Ding JR, Ding X, Hua B, Xiong X, Wen Y, Ding Z, Wang Q, Thompson P (2018) Altered connectivity patterns among resting state networks in patients with ischemic white matter lesions. Brain Imaging Behav 12:1239–1250 [PubMed: 29134612]
46. Whelton PK, Carey RM, Aronow WS, et al. (2017) ACC/AHA/AAPA/ABC/ACPM/AGS/APhA/ASH/ASPC/NMA/PCNA Guideline for the Prevention, Detection, Evaluation, and Management of High Blood Pressure in Adults: a Report of the American College of Cardiology/American Heart Association Task Force on Clinical Pr

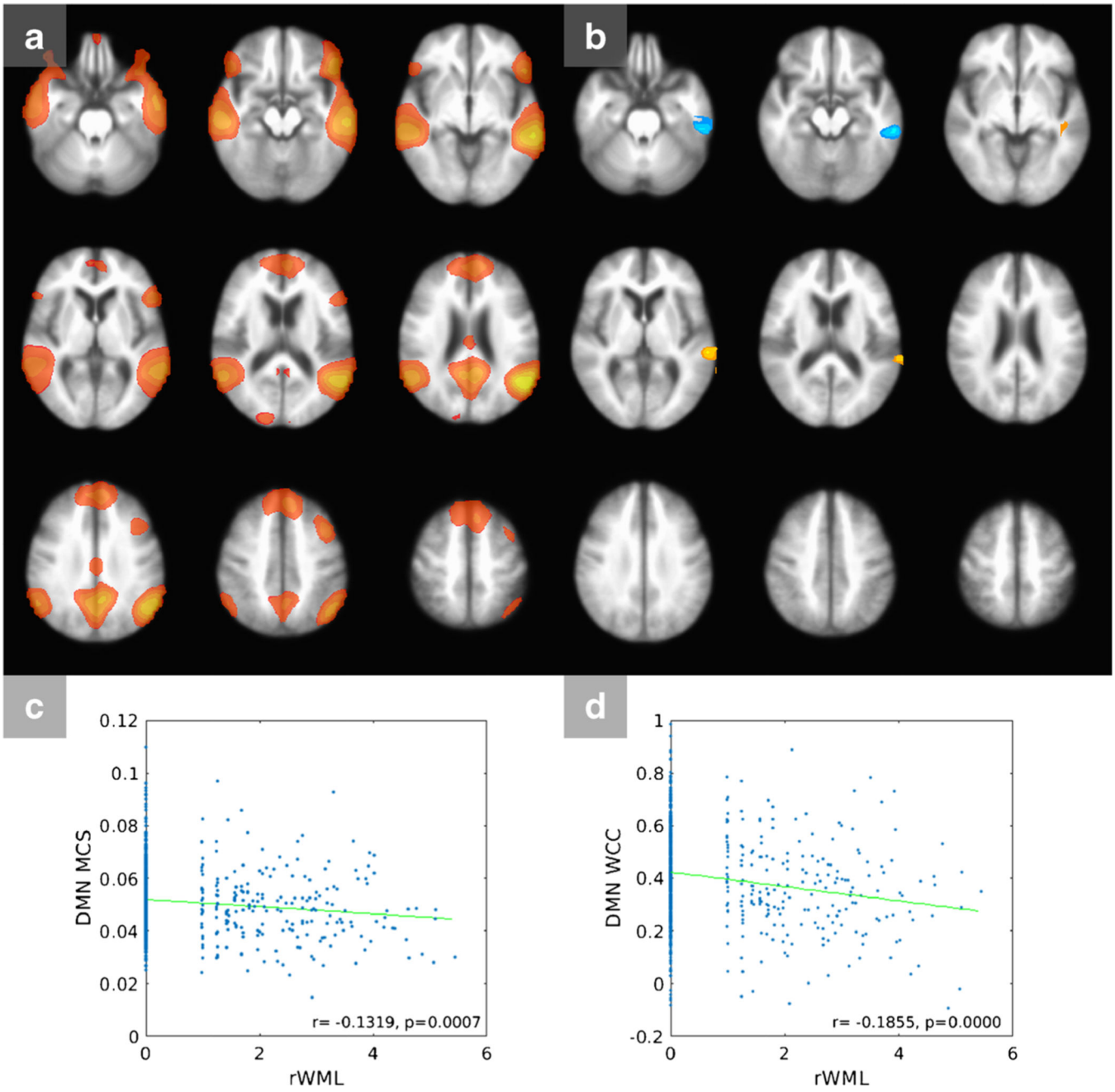

Fig. 1.

Default mode network (DMN). **a** Masked DMN map. **B** Connectivity—rWML correlation *t* map, indicating regions within the network where FC is correlated to rWML. Shades of red/yellow are positive and shades of blue are negative correlations. **c** Scatter plot of rWML vs. mean connectivity score. **d** Scatter plot of rWML vs. WML-related cluster connectivity. DMN, default mode network; MCS, mean connectivity score; rWML, regional white matter lesion volume; WCC, WML-related cluster connectivity

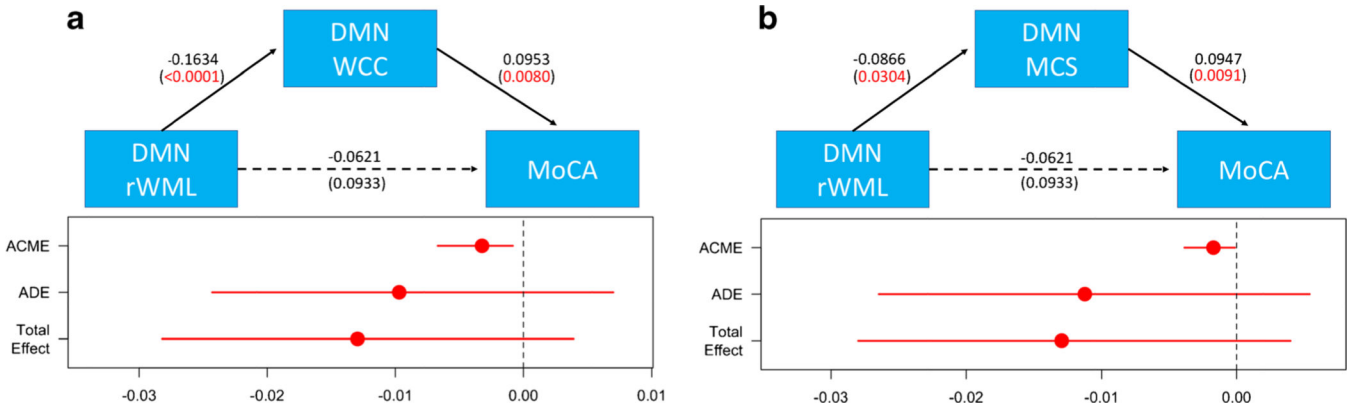

Fig. 2.

Results from mediation analysis. The conditional process diagrams present standardized β FC on rWML-cognitive relationships in the DMN. The mediating effects of both cluster connectivity (WCC, **a**) and mean connectivity (MCS, **b**) are provided. The average causal mediation effects (ACME), average direct effects (ADE), and total effect point estimates are shown, as are 95% confidence intervals. DMN, default mode network; MCS, mean connectivity score; rWML, regional white matter lesion volume; WCC, WML-related cluster connectivity; MoCA. Montreal Cognitive Assessment

Table 1

Characteristics of study cohort, $N = 660$

Demographic variables	
Age (years, mean ± SD)	68.3 ± 8.6
Female gender (N(%))	257 (38.9%)
Race (N(%))	
White	420 (63.6%)
Black	199 (30.1%)
Hispanic	30 (4.5%)
Other	11 (1.7%)
Clinical variables	
Systolic BP (mmHg), mean ± SD	138.6 ± 18.3
Diastolic BP (mmHg), mean ± SD	81.2 ± 12.4
# BP medications, mean ± SD	1.8 ± 1.0
eGFR (mL/min/1.73 m^2), mean ± SD	69.2 ± 21.2
Serum creatinine (mg/dL), mean ± SD	1.1 ± 0.4
Chronic kidney disease (eGFR < 60 mL/min/1.73 m^2) (N(%))	236 (35.8)
Structural imaging volumes (mean ± SD)	
Total gray matter volume (GM) (cm^3)	615.54 ± 65.09
Intracranial volume (ICV) (cm^3)	1391.02 ± 156.38
Gray matter ratio (GM/ICV)	0.44 ± 0.03
White matter lesion volume (mm^3)	4009.66 ± 6316.66

Table 2

White matter regions in which lesion volume is correlated with overall within-network connectivity for networks of interest

Network name	WM ROI name	*R*	*p* (uncorrected)	*p* (FDR-corrected)
ASLN	Posterior thalamic radiation	− 0.1354	0.0005	0.0231
ASLN	Genu of corpus callosum	− 0.1534	0.00007	0.0120
ASLN	Body of corpus callosum	− 0.1481	0.0001	0.0130
ASLN	Splenium of corpus callosum	− 0.1596	0.00003	0.0090
ASLN	Tapetum	− 0.1370	0.0004	0.0231
ASLN	Thalamus	− 0.1343	0.0005	0.0233
ASLN	Superior temporal WM	− 0.1319	0.0007	0.0269
DMN	Precuneus WM	0.1365	0.0004	0.0231
LFPN	Cingulum WM (Left)	− 0.1232	0.0015	0.0481
pDMN	Posterior corona radiata	− 0.1692	0.00001	0.0058
DFN	Fornix column and body	− 0.1408	0.0003	0.0224
BGN	Fornix column and body	− 0.1354	0.0005	0.0231

Only significant regions are displayed ($p < 0.05$, false discovery rate (FDR)–corrected).

ASLN, auditory-salience-language network; *BGN*, basal ganglia network; *DFN*, dorsal frontal network; *DMN*, default mode network; *LFPN*, left frontoparietal network;

Table 3

Multiple variable linear regression model statistics for cognitive test performance as a function of mean connectivity score. Each model was adjusted for gray matter ratio, age, gender, and race

Predictors	Cognitive test					
	MoCA		DSC		LM	
	Network MCS					
	Beta	*p* value	Beta	*p* value	Beta	*p* value
ASLN	6.0572	0.5505	71.867	0.0624	− 1.1639	0.8978
DMN	33.4727	*0.0025**	44.0752	0.292	10.2311	0.3006
LFPN	− 14.8289	0.2405	7.0492	0.883	− 0.8191	0.9421
Posterior DMN	− 22.9341	0.0909	12.5318	0.807	3.3826	0.78
DFN	− 6.4147	0.4131	− 45.2205	0.1276	− 1.6978	0.8085

* $p < 0.05$

ASLN, auditory-salience-language network; *DMN*, default mode network; *LFPN*, left frontoparietal network; *DFN*, dorsal frontal network; *MCS*, mean connectivity score; *MoCA*, Montreal Cognitive Assessment; *DSC*, Digit Symbol Coding test; *LM*, Logical Memory test

Table 4

Multiple variable linear regression model statistics for MoCA performance as a function of WML-related cluster connectivity. Each model was adjusted for gray matter ratio, age, gender, and race

Predictors	Cognitive test	
	MoCA	
	Beta	*p* value
FC (DMN WCC)	*2.1717*	*0.0040**
GMR	0.9269	0.874
Age	*− 0.1113*	*0.0000**
Gender	− 0.0053	0.9858
Race (White)	*2.778451*	*0.0091**
Race (Black)	− 0.5747	0.5963
Race (Hispanic)	− 0.8208	0.5168

* $p < 0.05$

DMN, default mode network; *GMR*, gray matter ratio; *WCC*, WML-related cluster connectivity; *MoCA*, Montreal Cognitive Assessment